Received: 25 September 2019 | Revised: 31 March 2020 | Accepted: 1 May 2020

DOI: 10.1002/stc.2586

RESEARCH ARTICLE

WILEY

Damage identification in frame structures using high-speed digital image correlation and local modal filtration

Ángel Jesús Molina-Viedma[1] | **Lukasz Pieczonka**[2] | **Krzysztof Mendrok**[2] | **Elías López-Alba**[1] | **Francisco A. Díaz**[1]

[1]Department of Mechanical and Mining Engineering, University of Jaén, Campus Las Lagunillas, Jaén, 23071, Spain

[2]Department of Robotics and Mechatronics, AGH University of Science and Technology, Al. Mickiewicza 30, Kraków, 30-059, Poland

Correspondence
Ángel Jesús Molina-Viedma, Department of Mechanical and Mining Engineering, University of Jaén, Jaén 23071, Spain.
Email: ajmolina@ujaen.es

Summary

This paper presents a technique for vibration-based damage detection and localization in engineering structures based on the high-speed three-dimensional Digital Image Correlation (HS 3D-DIC) and local modal filtration. The efficacy of the proposed procedure is demonstrated on a frame structure with different severities of localized damage. The full-field vibration data acquired under the white noise excitation provided the input to the damage identification algorithm. The spatial density of sensors on a test structure is one of the critical factors in the accurate localization of damage. Hence, the use of vision-based vibration measurement methods, such as the Digital Image Correlation (DIC) is very advantageous as it provides full-field quantification of dynamic displacement fields in three dimensions. Both numerical simulations with the use of Finite Element (FE) code and experimental tests with the use of high-speed digital cameras were performed to confirm the validity of the proposed approach. The research confirmed that it is feasible to use the proposed approach to detect and localize damage in a frame structure under random vibration excitation with a localization accuracy of a few percent of the field of view dimensions. On the basis of the obtained results, we believe that there is a great practical potential of this approach when applied to real-life engineering structures.

KEYWORDS

digital image correlation, frame structures, high-speed imaging, modal filtration, vibration-based damage detection

1 | INTRODUCTION

Maintaining structural integrity is of major concern for the mechanical and civil engineering structures alike. This problem is equally important for the new structures as well as for an existing aging infrastructure. Effective maintenance not only improves safety and the perception of safety but also minimizes the cost of ownership and mitigates unnecessary repairs. However, assuring the desired performance and safe operation of structures is not a trivial task. There are a large number of damage detection approaches that have been developed over the years, which could be used for this purpose.[1,2] Among them, the vibration-based damage detection methods which are arguably the most promising when it comes to the global assessment of structural health.[3–8] Vibration-based approaches are based on

the monitoring of changes of the modal properties of a structure. The presence of damage reduces the stiffness of a structure which affects its modal properties. Natural frequencies, damping factors, and mode shapes can all be used for damage detection purposes. Natural frequencies seem to be the best candidate for damage detection purposes as they are easy to measure with high precision. They are, however, also sensitive to environmental effects, and in practice, it is difficult to discern damage-induced alterations of natural frequencies from alterations caused by the environmental effects like temperature or humidity change. The uncertainty of experimental evaluation of damping ratios is typically high; therefore, they can be effectively used for damage detection purposes only in case of large damage severities. Finally, there are the mode shapes which can be measured accurately, and they are only moderately sensitive to the environmental changes. In addition, they provide spatial information about the investigated structure which is very important from the damage localization perspective. For this reason, mode shapes have been successfully used in the past for damage detection and localization purposes.[9–12] One of the particularly robust and effective methods in this group is based on the spatial analysis of modal filtration.[13–15] The practical limitation for the application of mode shape-based approaches is the required spatial density of sensors, especially for the techniques based on the mode shape derivatives.[16,17] In case of contact vibration sensors, this limitation can be both technical (i.e., mass loading of sensors and cables) as well as economical (i.e., costs rapidly increasing with the number measurement channels). These problems can be mitigated with use of noncontact vibration sensing techniques, especially with the rapidly developing vision-based methods.

Noncontact methods using local positioning[18,19] and vision systems[20,21] for vibration sensing are gaining attention for many civil and mechanical engineering applications related to Nondestructive Testing and Evaluation (NDT&E) and Structural Health Monitoring (SHM). Vision-based methods provide a global insight into the structures' dynamics eluding large and complicated instrumentation. Moreover, the spatial information is managed in a full-field manner, which could greatly benefit the efficiency of mode shape-based damage detection methods. Some studies performed laboratory test under controlled conditions. Feng and Feng[22] identified natural frequencies and mode shapes of a 1D beam using a vision sensor and validated them for cost-effective SHM. Wu et al.[23] performed 2D measurement on a reduced scale frame providing two approaches for improved calibration. Bridges or civil structures have been also under study using vision systems. In these works, different image processing methods for in-plane displacements were compared like 2D-DIC, pattern matching and edge detection[24] or also with a radar interferometer.[25] Pan et al.[26] developed a real-time system to measure vibration displacements in bridges by reducing image processing time.

The previous studies provide contactless measurements but do not take advantage of the full-field information because of employing optical targets to measure at discrete points. In this sense, Sarrafi et al.[27] employed phase-based motion estimation using complex steerable pyramid filters[28] for detecting changes in natural frequencies and full-field operational deflection shapes by additive masses in turbine blades. Fractal dimension was employed by Yang et al.[29] for reference-free damage location in mode shapes from phase-based motion estimation.

However, none of the mentioned methods are able either to perform 3D measurement; thus, they are limited to reduced cases. Conversely, the three-dimensional Digital Image Correlation (3D-DIC), which is one of the most robust and reliable techniques of vision-based vibration sensing, offers the possibility of measuring three spatial components of vibrations. This technique provides the characterization of 3D displacements in a full- field manner based on the 3D triangulation of the pattern recognition from stereovision.

The high frame rate performance of high-speed cameras allowed it to be employed in structural dynamics.[30] Particularly, many studies have explored the capabilities of this technique for modal analysis[31–33] and compared with traditional sensors, Scanning Laser Doppler Vibrometry (SLDV)[34–36] or Electronic Speckle Pattern Interferometry (ESPI).[37] Some studies have performed vibration and modal identification on rotating elements like discs[38] or helicopter blades.[39] According to limitations of this technique at high frequencies because of the displacement amplitude reduction, Molina-Viedma et al. studied the combination of phase-based motion magnification and 2D/3D-DIC especially to visualize higher frequency deflection shapes.[40,41] Motivated by the large amount of data generated in these studies, Chang et al.[42] performed a combination of compressed sensing and shape descriptors decomposition to compress DIC vibration data for operational modal analysis. They achieved an efficient methodology with significant compression ratio. Recently, Molina-Viedma et al.[43] performed a comparison of conventional 3D-DIC with an alternative single-camera version consisting of the combination of Fringe Projection and 2D-DIC (FP + DIC). The study evaluated the 3D modal response of a large aeronautical panel with both techniques. Despite the limitation of the single-camera system, it was proved a cost-efficient alternative for lower frequency analysis. In these studies, the lower sensitivity of the technique regarding sensors was evidenced, but, instead, the unprecedented spatial resolution was emphasized, what is especially relevant for mode shapes characterization. That makes the technique particularly attractive

for vibration-based damage detection. In a first approach, Felipe-Sesé and Díaz[44] developed a methodology for damage detection based on changes in full-field mode shapes measured by means of FP + DIC. However, localization of damage was not investigated.

The main novelty of this research study is the use of HS 3D-DIC combined with local modal filtration to detect and localize damage. Due to the very dense grid of measurement points obtainable by HS 3D-DIC, the analysis of accuracy of damage localization was performed depending on the measurement points group size used to build local modal filters. The efficacy of the approach is demonstrated in a laboratory frame structure with localized damage of different severities. Both numerical simulations and experimental measurements are used to demonstrate the efficacy of the proposed approach. The paper is organized in the following way: Section 2 discusses the theoretical background of the proposed approach including the applied modal filtration scheme and high-speed vision-based vibration sensing; Section 3 describes the test structure and its numerical model, followed by the results of damage detection and localization on simulated data; Section 4 discusses the experimental arrangements and test scenarios, followed by the presentation of experimental results; finally, the paper is concluded in Section 5.

2 | THEORETICAL BACKGROUND

2.1 | Modal filtration

The modal filter is a tool related to the modal model of a structure. It is a spatial filter that removes all structural modes from the frequency response of the system except the one to which the filter is set. Mathematically, this filtration is represented by the following formula:

$$\eta_r(\omega) = \psi_r{}^T \cdot \{x(\omega)\}, \tag{1}$$

where ψ_r is an rth reciprocal modal vector and $x(\omega)$ is a vector of system responses. The output characteristic of such a filter has only one peak related to the rth natural frequency to which the filter was tuned. Furthermore, the modal coordinates η_r may by scaled to a known input, and the FRF is calculated also with only one maximum value.

The idea to use a spatial filtration for damage localization was first described by Mendrok and Uhl[13-14] and Tondreau and Deraemaeker[15] as an extension of the damage detection algorithm based on modal filtration.[45–48] The modal filter was originally developed for the purpose of vibrations control.[49] Soon a number of other applications were found, such as identification of excitation forces, comparison of modal models, and structural health monitoring.[50] Deraemaeker and Preumont[48] used modal filtration for damage detection for the first time. Their idea was based on modal filtering of the frequency characteristics of the object in the current state with a modal filter coefficients identified with use of the data collected in the reference state. The method showed to have great potential due to several advantages, including the simplicity of calculations, low computing power required, data-based diagnosis (except the modal filter identification step), and the robustness against the change of external conditions. In addition, the results of this approach were easy to interpret. The method was further developed to allow its use for operational data.[46,47] A basic idea of modal filtration applied to damage detection is presented in Figure 1.

Modal filter coefficients are determined for the undamaged state (modal parameters indexed with n in Figure 1). Therefore, in this case, orthogonality holds between the relevant modal vectors and the selected modal filter coefficients. Hence, when the frequency characteristics of the object are subjected to modal filtration, the output shows a frequency characteristic with only one peak. When structure incurs damage, it results in the change of the modal parameters (indexed with d in Figure 1). The key issue here is the change of modal vectors, which are no longer orthogonal to the modal filter vectors. The lack of the orthogonality spoils the quality of the filtration and additional peaks appear in the output frequency characteristic.

The extension of this method for damage localization[13,14] takes into account the fact that damage, in most cases, only disturbs the mode shapes locally, which can be used for localization purposes. Therefore, the test structure is subdivided into multiple areas where vibrations are measured. Separate local spatial filters are built for data belonging to the specific areas of the sample. In the areas without damage, the shape of modes does not change significantly, and the modal filter maintains its filtering property. When a group of sensors located in the area of the damage is considered, mode shape is there disturbed, and the spatial filter does not perfectly filter the measured characteristics. The graphical presentation of this approach is presented in Figure 2.

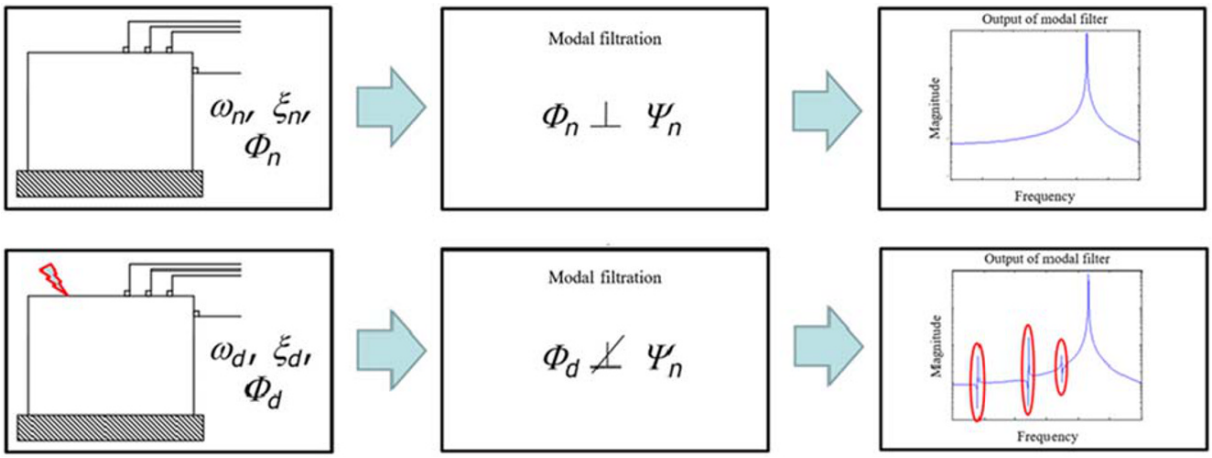

FIGURE 1 Idea of damage detection with modal filter. Upper row represents the reference undamaged case; lower row represents the damaged case

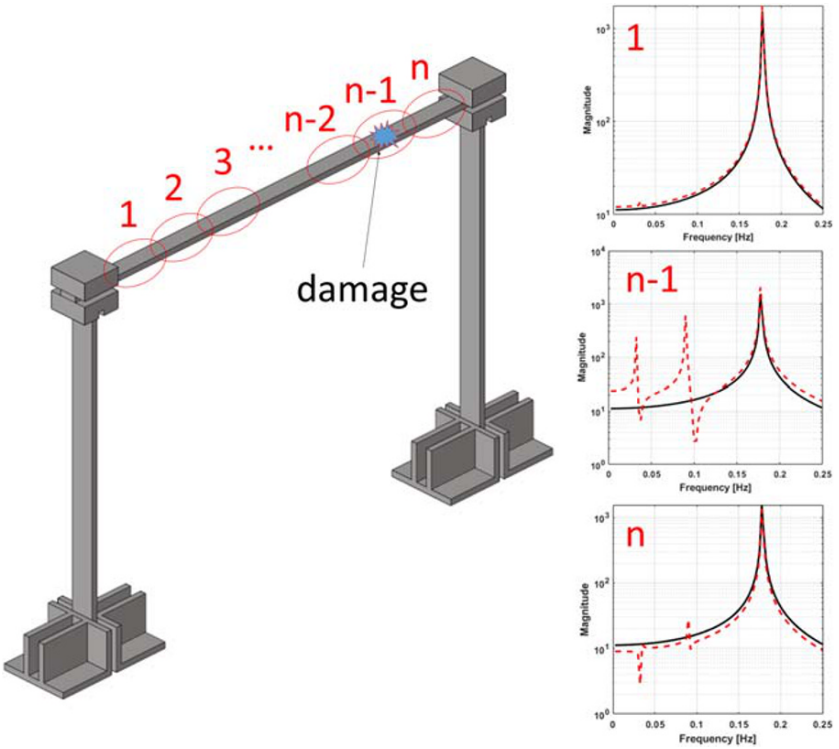

FIGURE 2 The concept of damage detection and localization using modal filtration. For a damage localized in section *n-1*, the quality of modal filtration deteriorated as opposed to healthy areas (e.g., *1* and *n*). Black solid line indicates the response of the modal filter in the reference state; solid dashed line indicates the response of the modal filter in the damaged condition

In order to parameterize the damage localization results, the Damage Index (DI) was introduced. It is provided by Equation 2:

$$\mathrm{DI} = \frac{\int_{\omega_s}^{\omega_f} \left| x_i(\omega) - x_{ref}(\omega) \right|^2 d\omega}{\int_{\omega_s}^{\omega_f} x_{ref}(\omega)^2 d\omega}, \tag{2}$$

where ω_s is the lower limit of the analyzed frequency band, ω_f is the upper limit of the analyzed frequency band, x_i is the frequency response in the current state, and x_{ref} is the frequency response in the reference state.

The DI is computed only for the frequency bands directly surrounding the natural frequencies of the monitored object, except the one to which the spatial filter is tuned. Typically, the width of the consecutive frequency intervals amounts to 10–50 spectral lines on both sides of the natural frequency (depending on the damping coefficient and frequency resolution of the measurements). For convenience of interpretation, the results are frequently presented in

the form of bar charts, where the amplitude of successive bars indicates the DI value for the subsequent groups of sensors (areas).

It has been proved in Zhang et al.[50] that the minimum number of sensors required to formulate an effective modal (spatial) filter is equal to or greater than the number of mode shapes in the frequency band of interest. Thus, by limiting the frequency band of the analysis to the first two mode shapes, it would be possible to build filters for areas covered with only two sensors. This would increase the accuracy of damage localization. In practice, however, to construct the modal filter for two modes, the data from at least four sensors have to be used.[14] The accuracy of damage localization depends then on the measurement grid density. In the case of using conventional sensors, e.g., accelerometers, this results in a significant increase in monitoring costs or a loss of system spatial resolution. The use of full-field vision-based measurements alleviates these limitations and offers a great potential for damage detection purposes.

2.2 | High-speed three-dimensional digital image correlation

Digital Image Correlation (DIC) is an optical technique that provides full-field displacements from a set of digital images.[51,52] It performs a tracking through the image sequence of small squared areas, as a result of dividing the region of interest, known as facets (Figure 3). The tracking is based on the correlation of the intensity of light of the facets after loading with respect to the reference image, as they are displaced and deformed as a consequence of the structure deformation. Therefore, the facet whose central pixel is P in the reference image is identified in the subsequent images by finding that pixel whose facet yields the maximum correlation coefficient. As a result of performing the correlation procedure for every facet, a map of displacements is obtained with a high spatial density. To enable the tracking, every facet must have an unequivocal and distinct intensity distribution; thus, the specimen surface is commonly coated with black and white paint to generate a gray scale random pattern known as speckle.

Under this basis, two measurement scenarios are possible, depending on the desired dimensionality of the vibration sensing. The 2D version is employed for in-plane measurements using a single camera and only a pixel-mm factor is required for calibration. Including a second camera for stereovision, a 3D analysis can be performed. In this case, a more complex calibration is required consisting in both intrinsic parameters and extrinsic parameters that represent the relative location, t, and orientation, R, of both cameras and a common world coordinate system, as illustrated in Figure 3b.

High-speed cameras have spread the field of application of DIC to a wide range of dynamic events. Providing frame rates of the order of thousands frames per second (fps) with maximum image resolution, high-speed cameras make it suitable for vibration and modal analysis of a wide variety of structures with resonance frequencies in such a frequency range. Therefore, vibration-based damage detection can also be explored.

3 | TESTS STRUCTURE AND FINITE ELEMENT MODELING

The test sample was a bolted frame structure depicted schematically in Figure 4. The overall dimensions of the frame were 1,000 × 660 × 120 mm. The frame was composed of two vertical steel beams with cross-sectional dimensions of

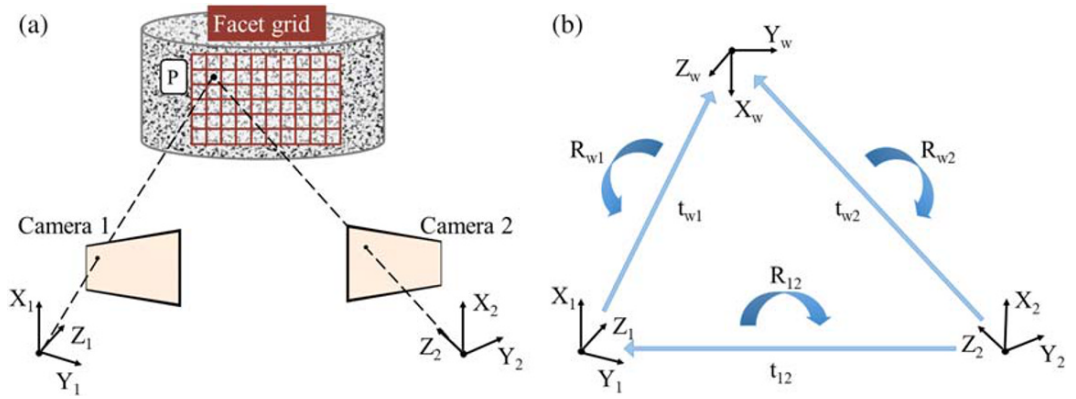

FIGURE 3 (a) Schematic of the optical arrangement for 3D-DIC measurement. (b) Transformation between cameras 1 and 2 and the world coordinate system, w

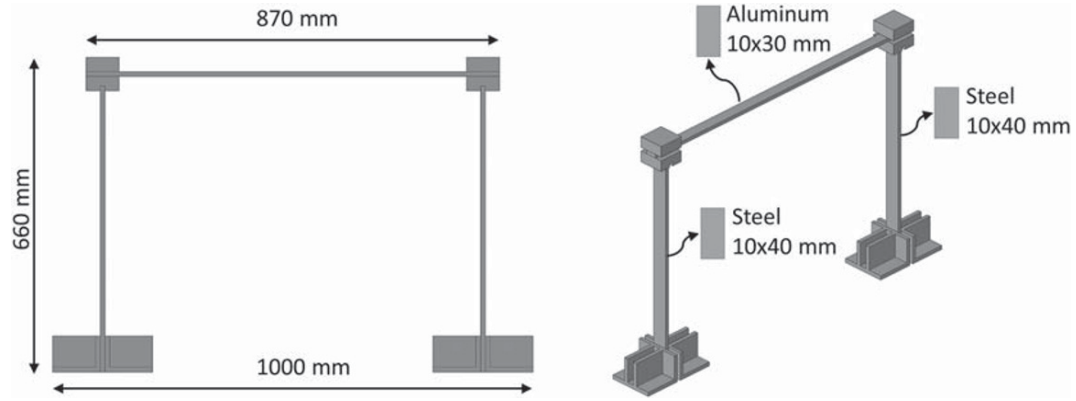

FIGURE 4 Schematic of the analyzed frame structure

10 × 40 mm and the total length of 590 mm and a horizontal aluminum beam with cross-sectional dimensions of 10 × 30 mm and the total length of 870 mm. The beam members were clamped with steel blocks and bolted together. The base of the frame was fixed to the ground by eight bolts, four for each of the feet.

Based on the geometrical model of the test structure, a numerical model was prepared in order to perform initial analyses of the mode shapes for reference and damaged conditions. The goal of this exercise was to verify the validity of the modal filter-based damage localization in the idealized case of noise-free mode shape data. In addition, the numerical simulations were used to evaluate the influence of the localization algorithm parameters (such as the choice of the mode shape and size of the sensors group) on the performance of damage detection and localization.

The geometry of the frame was modeled using *MSC. Patran* FE preprocessor and discretized using 40,000 3D linear hexahedral elements. The model is shown in Figure 5. The analysis involved the following material parameters:

- Material 1: $E = 210$ GPa, $\nu = 0.30$, $\rho = 7.85$ g/mm^3,
- Material 2: $E = 70$ GPa, $\nu = 0.33$, $\rho = 2.7$ g/mm^3,

where E is the Young's modulus, ν is the Poisson's ratio, and ρ is the density.

Material 1 was assigned to the vertical and connection elements of the frame, whereas material 2 was assigned to the horizontal frame member. Damage in the horizontal member was modeled by removing from the model a row of finite elements along the X-axis as shown in Figure 5. There were six elements across the thickness of the beam; therefore, removing a single row of elements resulted in a 1.67 mm (∼17%) thickness reduction. This can be seen in

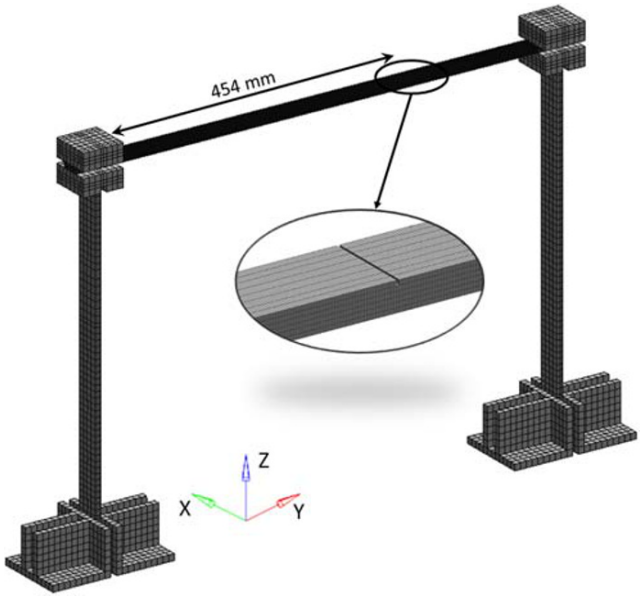

FIGURE 5 Schematic of the numerical model demonstrating the location of simulated damage

the insert in Figure 5. Removal of subsequent rows of finite elements resulted in thickness reductions of 34% and 50%, respectively. The notch was located at the distance of 454 mm from the left end of the beam as shown in Figure 5.

Natural frequencies and mode shapes of the frame were obtained by solving the free undamped vibration problem. The equations of motion can be formulated as

$$[M]\{\ddot{u}\} + [K]\{u\} = 0, \tag{3}$$

where $[M]$ is the mass matrix, $[K]$ is the stiffness matrix, $\{u\}$ is the displacements vector, $\{\ddot{u}\}$ is the accelerations vector.

Equation 3 can be solved assuming the solution of the form

$$\{u\} = \{\phi\} \sin \omega t, \tag{4}$$

where $\{\phi\}$ is an eigenvector and ω is the circular natural frequency of vibration. Substituting Equation 4 to Equation 3 yields

$$-\omega^2[M]\{\phi\}\sin(\omega t) + [K]\{\phi\}\sin(\omega t) = 0, \tag{5}$$

This can be rewritten in a simplified form as

$$([K] - \omega^2[M])\{\phi\} = 0, \tag{6}$$

It is well-known that the above set of equations can be satisfied when $\{\phi\} = 0$ or when $|[K] - \omega^2[M]| = 0$. The former is a trivial solution, representing the case when no motion occurs. The latter can be investigated to find the solutions. The determinant $|[K] - \omega^2[M]|$ becomes zero at a discrete set of eigenvalues ${\omega_i}^2$ that are accompanied by the corresponding eigenvectors $\{\phi_i\}$. Each pair of eigenvalue and eigenvector represents a free undamped vibration mode of the plate. The frequency of vibration f_i equals $\omega_i/2\pi$. The eigenvectors $\{\phi_i\}$ are mutually orthogonal meaning that vibration mode shapes described by the eigenvectors are unique and cannot be described by a linear combination of other mode shapes. The mode shapes that are calculated are arbitrarily scaled, as there is no forcing on the right hand side of Equation 3. The work presented in this paper assumes the mass normalization of eigenvectors, i.e., the eigenvectors, fulfill the formula

$$\{\phi_i\}[M]\{\phi_i\} = 1, \tag{7}$$

Several techniques can be applied for the solution of an eigenproblem. In the present study, the Lanczos algorithm was applied, as it is proven to accurately compute a discrete set of eigenvalues and eigenvectors for medium and large size FE models. It is also important to note that the algorithm used does not miss any roots and offers very good numerical performance.

The *MSC.Nastran* FE solver was used to perform computations. The normal modes solution (SOL103) was applied to find vibration mode shapes of the frame in both damaged and undamaged state.

3.1 | Damage identification using modal filtration

The analysis was performed for the lowest damage severity, i.e., when only one row of nodes was removed resulting in 17% thickness reduction. A line of nodes placed in the middle of the horizontal beam width on their upper surface was selected for the calculations. Only vibrations in the vertical Z direction were analyzed. For localization purposes, nodes were grouped without overlapping. Four different scenarios were considered with group sizes of 50, 30, 15, and 5 points respectively. Mesh density along the length of the beam was equal to 1 mm; therefore, the group sizes were equivalent to the spatial filter sizes expressed in millimeters.

In the first step, the analysis of the influence of the mode shape number to which the modal filter was tuned on the localization effectiveness was performed. The results of these analyses considering the group size of five nodes are presented in Figure 6.

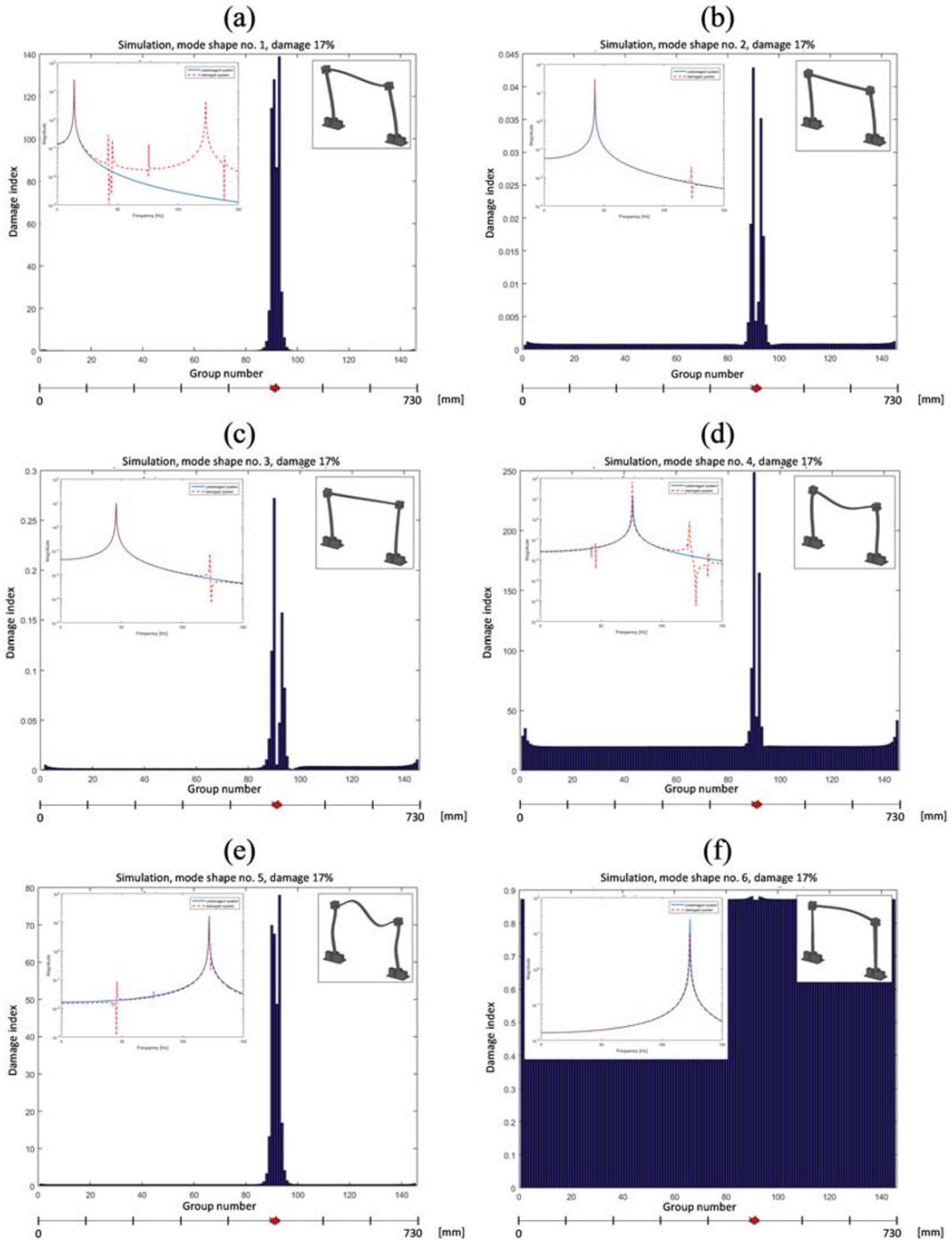

FIGURE 6 Results of the modal filter based damage localization for different choices of filtered mode shapes. Figures from *a* to *f* represent mode shapes from 1 to 6, respectively. The inserts in the top left corner show the modal filter response for an undamaged frame (solid blue line) and for the damaged frame (dashed red line). The inserts in the top right corner present the associated mode shapes. The scale at the bottom of each figure shows the actual span of the horizontal beam member with damage indicated with the red marker

The analysis indicated that the modal filter tuned to the first mode shape gives the best results. The value of damage index DI is high; the elevated DI level is present only around the damage location, and it provides an accurate localization of damage (without splitting). Positive results were also returned by filters tuned to modes number 4 and 5. Also, in these cases, it can be attributed to the associated mode shape involving bending of the horizontal beam member in the YZ plane where the damage was introduced. The filters tuned to modes 2 and 3 provided an indication of the location of damage; however, the values of the DI are very low. Most likely in the presence of measurement noise, these

modes would not yield satisfactory results. Finally, the modal filter tuned to mode number 6 was not sensitive to this type and location of damage at all. The results were also consistent for larger damage severities (34% and 50% thickness reduction) considered in the model. Therefore, modal filters tuned to mode number 1 were used for further numerical and experimental analyses.

In the next step, the localization accuracy was studied as a function of the number of nodes in a group. As mentioned earlier, group sizes of 50, 30, 15, and 5 nodes were considered. The group sizes were equivalent to the spatial filter sizes expressed in millimeters, because of the mesh density equal to 1 mm. The results of the analysis are summarized in Figure 7. Damage indicator bar plots are plotted for each of the considered group sizes; red vertical curve in the plots indicates the true location of damage. In all cases, the localization of damage is unequivocal; however, the precision of localization increases with the decrease of the group size. For modal filters constructed with 50 points in a group, we can identify the location of damage in the region of the nonzero values of the DI (bins number 9 and 10) that is between 400 and 500 mm, whereas the true location of damage was at the distance of 454 mm. The peak of the DI is shifted to the right with respect to the true location of damage, which can be attributed to the fact that the mode shape after introducing damage does not change symmetrically, which is revealed by the local DI values. For

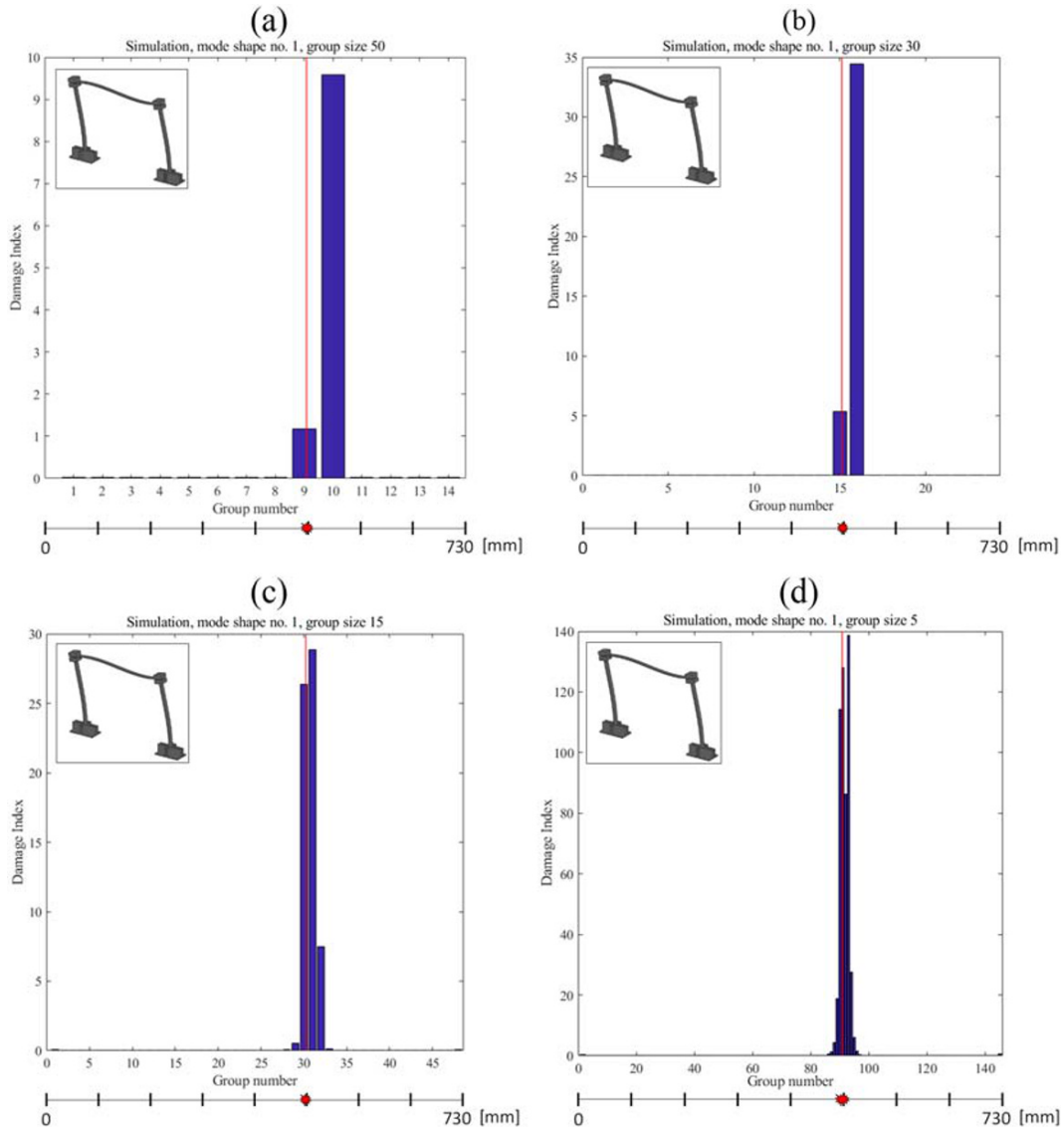

FIGURE 7 Damage localization accuracy as a function of the group size used to construct the modal filter: (a) 50 points, (b) 30 points, (c) 15 points, and (d) 5 points. The analysis was performed for the first mode shape shown in the inserts in the top left corner of each figure. The scale at the bottom of each figure shows the actual span of the beam member with damage indicated with the red marker

modal filters constructed with 30 points in a group damage, the same pattern holds indicating the location of damage between 420 and 480 mm. For modal filters constructed with 15 points in the location, damage can be identified between 435 and 480 mm. Finally, for modal filters constructed with 5 points in a group, the location damage can be identified between 440 and 470 mm. The analysis indicates that for the case under consideration, starting from the size of group 15, the accuracy of damage location does not increase. In all cases, the highest peak is shifted to the right-hand side with respect to the true location of the damage. The mode shape area disturbed by the damage is much larger than the damage itself, and this determines the accuracy of the localization.

4 | EXPERIMENTAL INVESTIGATION

For the application of damage identification using modal filtration, a modal identification using HS 3D-DIC was performed. The test structure was excited laterally using an electrodynamic shaker, as shown in the Figure 8, with a white noise signal bandpass filtered from DC to 256 Hz. The response of the horizontal member was monitored by two high-speed cameras model Phantom v9.1. The focus was placed on the frontal surface of the horizontal beam member. Despite the predominant in-plane motion of the frame, the 3D system was set to perform the general measurement case. Images were recorded at a frame rate of 512 fps with 400 ms (1/2,500 s) of exposure time. A load cell was employed to monitor the excitation. The acquisition was synchronized with the cameras by connecting the signal generator with the camera controller.

3D-DIC was employed to infer the deformation experienced by this member during the excitation. According to the technique's requirement for accurate measurements,[51] a random pattern was painted based on black speckles with a white background. The region of interest was divided in facets of 11 pixels size and employing an overlap step of 2 pixels, each of which represents a measurement point. Considering the predominant bending behavior of the member, vertical displacements were only investigated. To reduce redundant information and make it a 1D problem, a vector of spatial measurements were obtained by averaging along the thickness, assuming negligible variations in that direction. As a result, the beam was experimentally modeled as line of 675 points, resulting 1.08-mm spacing.

Measurements were performed in the frame structure in both undamaged and damaged states. Different damage severities were made as a transversal notch in the upper face. Three different depths of the notch were considered, namely, 0.8, 2.5, and 4 mm, which were equivalent to 8%, 25%, and 40% thickness reduction, respectively. Similarly to the simulated case, the notch was located 454 mm away from the top left clamp, as shown in Figure 5. The size of groups for local modal filters was selected in such a way that their spatial dimensions were comparable with these of simulation.

The time histories of vertical displacements were evaluated along with the force signal to infer the modal behavior of the horizontal beam member. Based on the processed time domain data, the Frequency Response Functions (FRFs) were estimated using the VIOMA toolbox.[7] The following processing parameters were used: estimator, H1; time window, Hann; frequency resolution, 0.5 Hz; overlapping, 50%; number of averages, 11. The calculated frequency domain data for the undamaged frame and the subsequent damage stages were used as the basis for modal filtration.

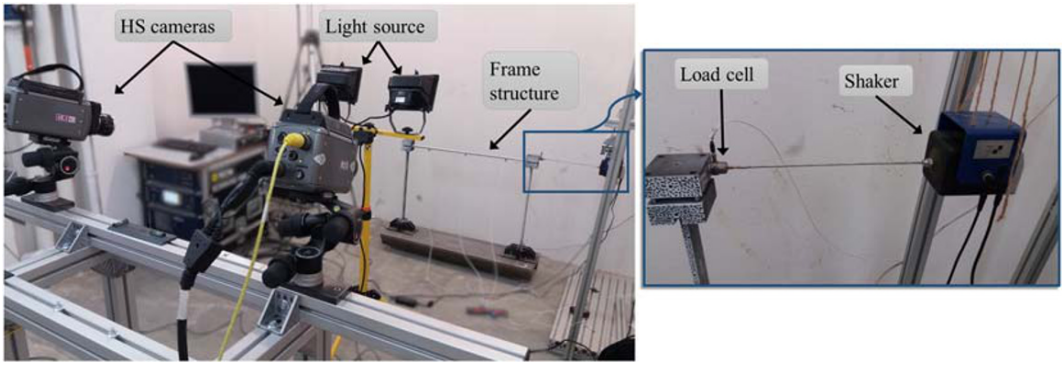

FIGURE 8 Experimental setup for HS 3D-DIC measurement under white noise random excitation

4.1 | Results

Damage detection and localization were performed based on the acquired and processed high-speed DIC full-field measurements. In the frequency band from 0 to 256 Hz, five resonant modes were identified, of which the first mode at 12.61 Hz was selected for damage detection and analysis as indicated by the numerical study. In the first step, it was assumed that the size of the local modal filters will be equal to 20 measurement points. This allowed to compile 33 groups of virtual sensors. The size of each group was equal to approximately 22 mm. Figure 9 shows the results of damage localization using this configuration for the subsequent damage stages from 0.8 mm through 2.5 mm to the final depth of 4 mm.

As can be seen in Figure 9, damage can be correctly localized at all levels by looking at the peak value of the DI. For all levels of damage, the increased value of the damage index occurs in group number 24, i.e., slightly to the right-hand side from the actual location of the damage indicated by the vertical red line in each figure. This phenomenon can also be observed for simulation data and results from the way the mode shape changes under the influence of the notch. For

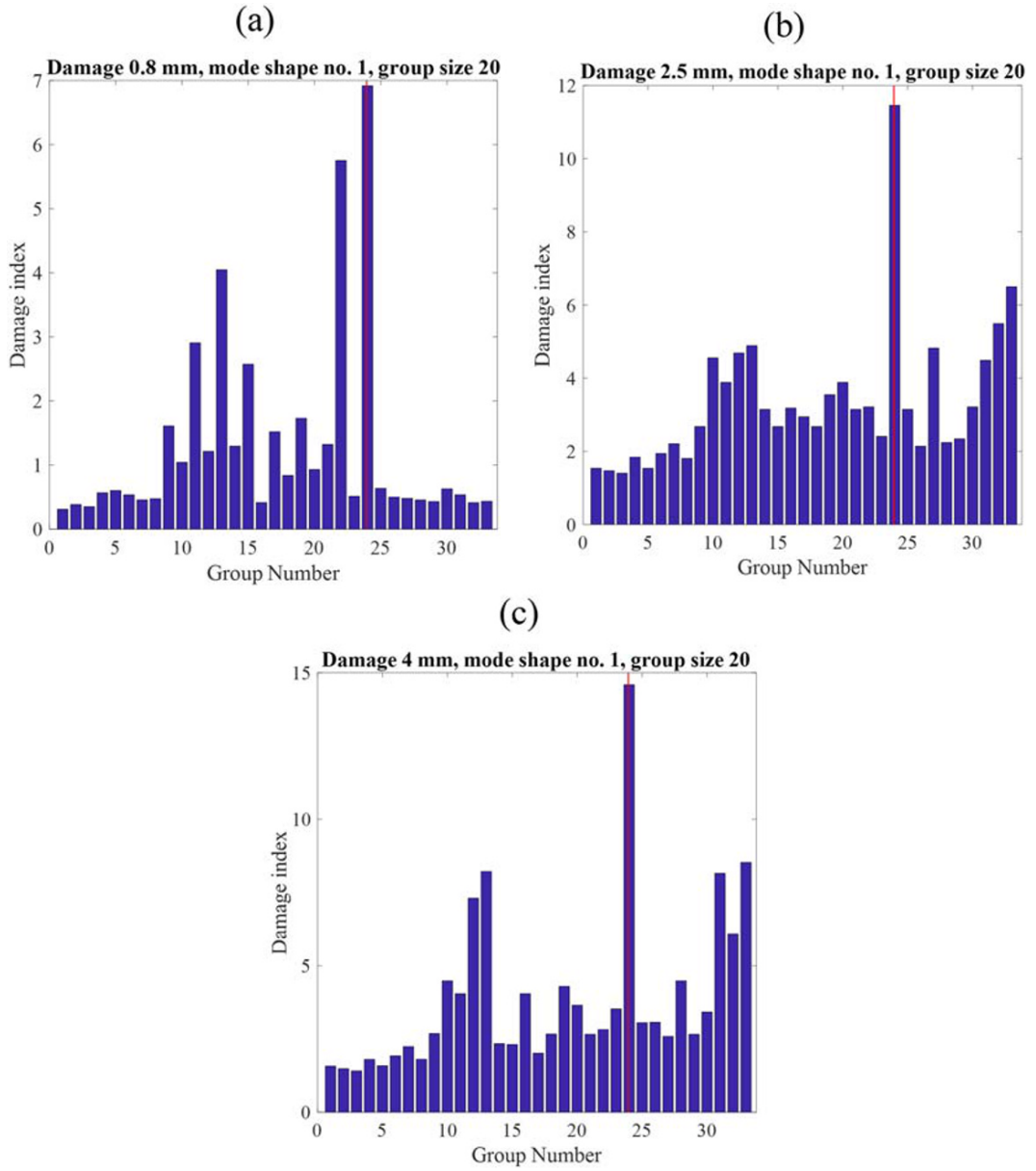

FIGURE 9 Results of the damage detection and localization process for the consecutive damage levels: (a) 0.8 mm, (b) 2.5 mm, and (c) 4 mm. Local modal filter applied with 20 measurement points in a group. Red vertical lines in the figures indicate the true position of damage

the most shallow cut (0.8 mm), there is an additional peak in bin number 22, but with larger severities of damage, the localization becomes more unequivocal.

To increase the resolution of damage localization, the number of virtual sensors in each group was reduced to 10. This results in the spatial span of each group of approximately 11 mm and the total number of groups equal to 66. The results of damage detection and localization for this configuration and the consecutive damage levels are presented in Figure 10.

For this group size, the indication of damage location is even more precise. It should be noted, however, that the number of groups for which the DI values significantly exceed the background level also increased. These high values of the DI are present also away from the true location of damage, which can be attributed to the presence of measurement noise which is more influential for the smaller group sizes.

Finally, the analysis was carried out for a group size of 5 measurement points, equivalent to a filter size of 5.5 mm. The results of damage detection and localization for this case and for the consecutive damage levels are shown in Figure 11.

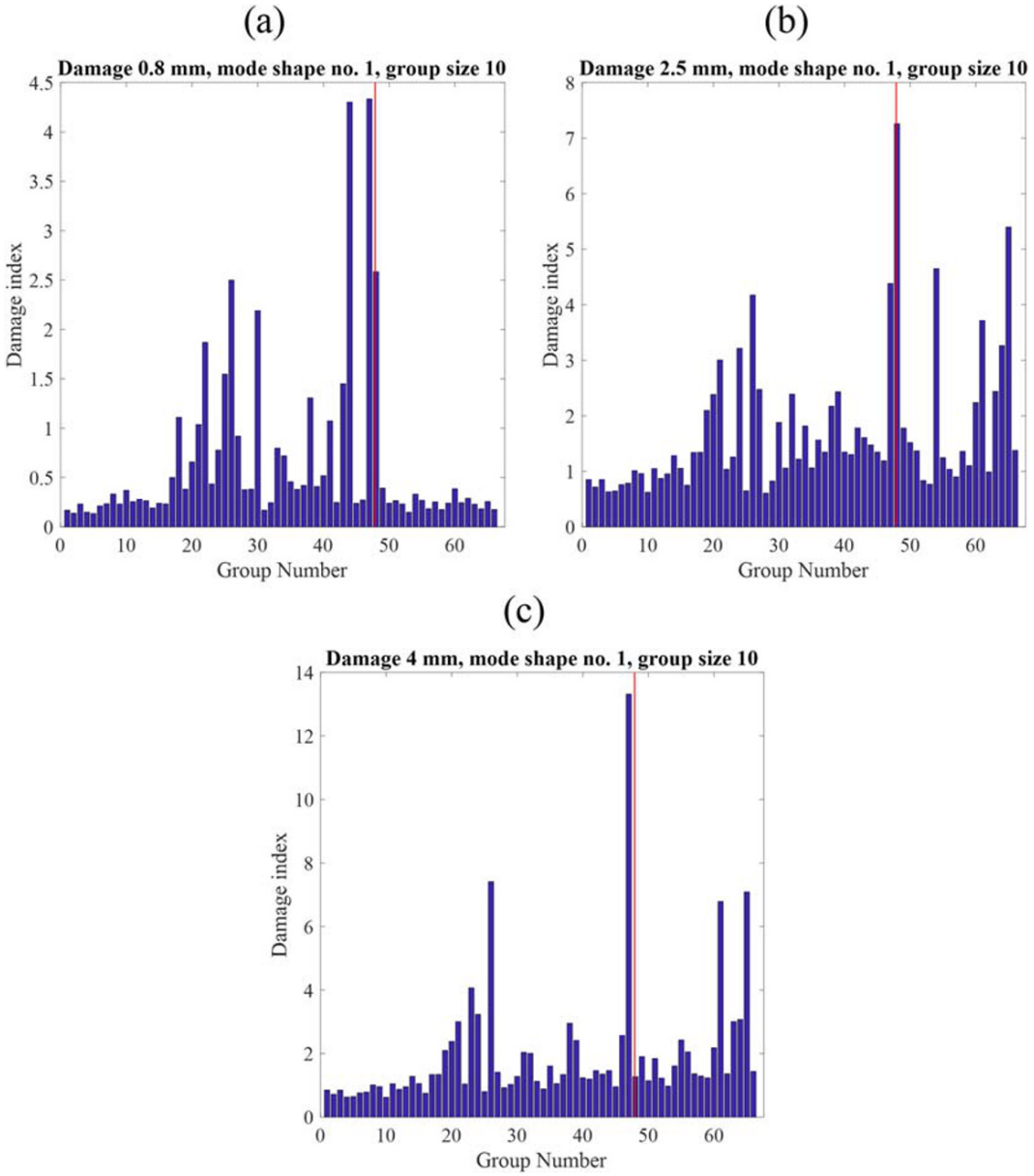

FIGURE 10 Results of the damage detection and localization process for the consecutive damage levels: (a) 0.8 mm, (b) 2.5 mm and (c) 4 mm. Local modal filter applied with 10 measurement points in a group. Red vertical line in the figures indicates the true position of damage

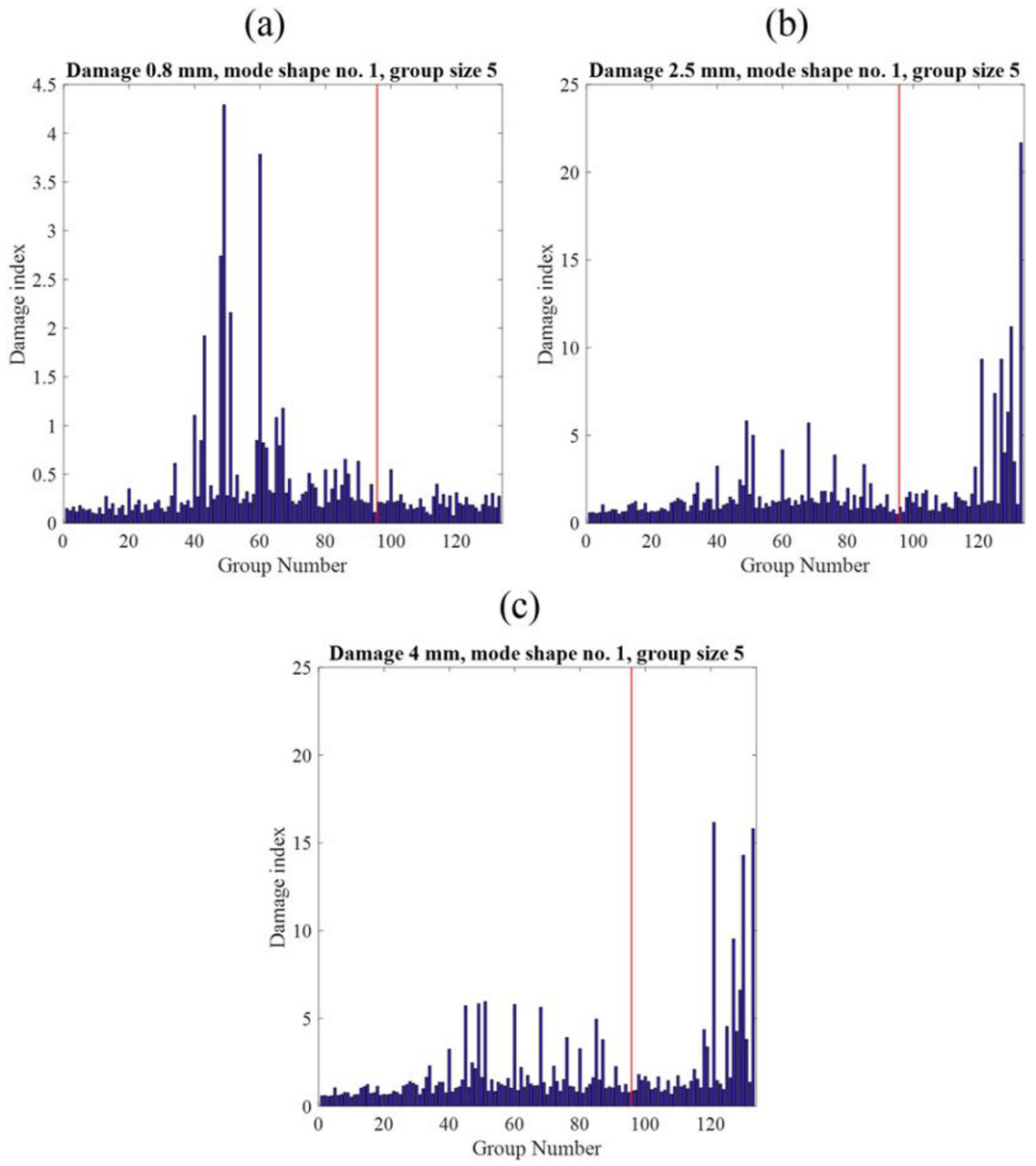

FIGURE 11 Results of the damage detection and localization process for the consecutive damage levels: (a) 0.8 mm, (b) 2.5 mm, and (c) 4 mm. Local modal filter applied with 5 measurement points in a group. Red vertical line in the figures indicates the true position of damage

In this case, the total number of groups was 133. As can be seen, in this case, the localization was not successful and even the largest severity of damage could not be detected. This is on the contrary to the simulated data where local modal filters with 5-mm spatial size were still providing correct results. This fact can be attributed to the presence of measurement noise which was absent in the numerical data. As expected, the effect of measurement noise is more pronounced for the lower group sizes used to construct local modal filters. This could be potentially improved in the experimental data by lengthening the image registration time and allowing for more averaging. Ultimately, however, the measurement noise will always be the decisive factor when comes to the reduction of the spatial filter size and the precision of damage localization.

5 | CONCLUSIONS

In this paper, we have discussed the theoretical and experimental framework for damage detection and localization in engineering structures based on the high-speed digital image correlation and local modal filtration. We have

demonstrated, both numerically and experimentally, that it is feasible to use local modal filters in combination with full-field vibration measurement to detect and localize damage in a nontrivial case of a buildup frame structure. The method is based on the retrieval of full-field vibration data using digital image correlation of a high-speed video sequence acquired under the random vibration excitation, which is of high practical relevance. Local modal filtration allows not only to detect but also to localize damage in a structure with the accuracy dependent on the spatial size of the applied modal filter.

We have demonstrated that the proposed approach can be successfully used in experiments to detect and localize damage ranging from 8% to 40% of the cross section of a beam member. The choice of the size of the local modal filter determines not only the precision of damage localization but also the sensitivity to the measurement noise. In the case of simulated data free from the noise, size of the local modal filter can be reduced to only a few measurement points allowing for very precise localization of damage. In the case of experimental data, reduction of the spatial dimension of the local modal filter is limited by the increasing influence of the measurement noise, as expected. Nonetheless, the accuracy of damage localization down to a few millimeters can be achieved for a measurement area of approximately 1 m^2 with the available high-speed cameras.

On the basis of the results reported in this study, we believe that the proposed approach has a great potential for practical engineering applications. Further investigations are planned to verify the effectiveness of this approach on large scale engineering structures and in case of multiple localized damages.

ACKNOWLEDGEMENTS

The authors would like to acknowledge Piotr Kohut and Krzysztof Holak for their advice and technical support with DIC experiments.

ORCID

Ángel Jesús Molina-Viedma https://orcid.org/0000-0002-5425-7683
Lukasz Pieczonka https://orcid.org/0000-0003-3623-3984

REFERENCES

1. Moore PO (Ed). *Nondestructive Testing Handbook*. 3rd ed. American Society for Nondestructive Testing; 2012.
2. Stepinski T, Uhl T, Staszewski W, Eds. *Advanced Structural Damage Detection: From Theory to Engineering Applications*. 2013.
3. Fan W, Qiao P. Vibration-based damage identification methods: a review and comparative study. *Struct Health Monit: Int J*. 2011;10(1):83-111. https://doi.org/10.1177/1475921710365419
4. Pieczonka L. Vibration-based structural health monitoring and damage detection considering uncertainties in model parameters and in experimental data 2010.
5. Dworakowski Z, Kohut P, Gallina A, Holak K, Uhl T. Vision-based algorithms for damage detection and localization in structural health monitoring. *Struct Control Health Monit*. 2016;23(1):35-50. https://doi.org/10.1002/STC.1755
6. Tributsch A, Adam C. An enhanced energy vibration-based approach for damage detection and localization. *Struct Control Health Monit*. 2018;25(1):1-16. https://doi.org/10.1002/stc.2047
7. Uhl T, Lisowski W, Kurowski P. *In-operation modal analysis and its applications*. Krakow (Poland): AGH Publishers; 2001.
8. Lisowski M, Gonek P, Korta J, Uhl T, Staszewski WJ. Structural damage detection using wireless passive sensing platform based on RFID technology. *Struct Control Health Monit*. 2016;23(8):1135-1146. https://doi.org/10.1002/stc.1826
9. Ho YK, Ewins DJ. Numerical Evaluation of Damage Index. In: Chang FK, ed. *Structural health monitoring 2000: proceedings of the 2nd International Workshop on Structural Health Monitoring*. Stanford, CA; 1999.
10. Carrasco CJ, Osegueda RA, Ferregut CM, Grygier M. Damage localization in a space truss model using modal strain energy. Proceedings of the 15th International Modal Analysis Conference (IMAC) Part 2 (of 2), 2, 1997.
11. Kohut P, Kurowski P. The Integration of Vision System and Modal Analysis for SHM Application. Proceedings of the 24th International Modal Analysis Conference (IMAC), 2006.
12. Porcu MC, Patteri DM, Melis S, Aymerich F. Effectiveness of the FRF curvature technique for structural health monitoring. *Construct Build Mater*. 2019;226:173-187. https://doi.org/10.1016/j.conbuildmat.2019.07.123
13. Mendrok K, Uhl T. Modal filtration for damage detection and localization. Proceedings of the 4th European Workshop on Structural Health Monitoring, 2008.
14. Mendrok K, Uhl T. Experimental verification of the damage localization procedure based on modal filtering. *Struct Health Monit*. 2011;10(2):157-171. https://doi.org/10.1177/1475921710373292
15. Tondreau G, Deraemaeker A. Local modal filters for automated data-based damage localization using ambient vibrations. *Mech Syst Signal Process*. 2013;39(1–2):162-180. https://doi.org/10.1016/j.ymssp.2013.03.020
16. Pandey AK, Biswas M, Samman MM. Damage detection from changes in curvature mode shapes. *J Sound Vib*. 1991;145(2):321-332. https://doi.org/10.1016/0022-460X(91)90595-B

17. Moreno-García P, Araújo dos Santos JV, Lopes H. A new technique to optimize the use of mode shape derivatives to localize damage in laminated composite plates. *Compos Struct*. 2014;108:548-554. https://doi.org/10.1016/j.compstruct.2013.09.050
18. Casciati F, Wu L. Local positioning accuracy of laser sensors for structural health monitoring. *Struct Control Health Monit*. 2013;20(5):728-739. https://doi.org/10.1002/stc.1488
19. Wu L, Casciati F. Local positioning systems versus structural monitoring: a review. *Struct Control Health Monit*. 2014;21(9):1209-1221. https://doi.org/10.1002/stc.1643
20. Ye XW, Dong CZ, Liu T. A review of machine vision-based structural health monitoring: methodologies and applications. *J Sensor*. 2016;2016:1-10. https://doi.org/10.1155/2016/7103039
21. Feng D, Feng MQ. Computer vision for SHM of civil infrastructure: from dynamic response measurement to damage detection—a review. *Eng Struct*. 2018;156:105-117. https://doi.org/10.1016/j.engstruct.2017.11.018
22. Feng D, Feng MQ. Experimental validation of cost-effective vision-based structural health monitoring. *Mech Syst Signal Process*. 2017;88(November 2016):199-211. https://doi.org/10.1016/j.ymssp.2016.11.021
23. Wu LJ, Casciati F, Casciati S. Dynamic testing of a laboratory model via vision- based sensing. *Eng Struct*. 2014;60:113-125. https://doi.org/10.1016/j.engstruct.2013.12.002
24. Cigada A, Mazzoleni P, Zappa E. Vibration monitoring of multiple bridge points by means of a unique vision-based measuring system. *Exp Mech*. 2014;54(2):255-271. https://doi.org/10.1007/s11340-013-9784-8
25. Kohut P, Holak K, Uhl T, et al. Monitoring of a civil structure's state based on noncontact measurements. *Struct Health Monit: Int J*. 2013;12(5–6):411-429. https://doi.org/10.1177/1475921713487397
26. Pan B, Tian L, Song X. Real-time, non-contact and targetless measurement of vertical deflection of bridges using off-axis digital image correlation. *NDT E Int*. 2016;79:73-80. https://doi.org/10.1016/j.ndteint.2015.12.006
27. Sarrafi A, Mao Z, Niezrecki C, Poozesh P. Vibration-based damage detection in wind turbine blades using phase-based motion estimation and motion magnification. *J Sound Vib*. 2018;421:300-318. https://doi.org/10.1016/j.jsv.2018.01.050
28. Wadhwa N, Rubinstein M, Durand F, Freeman WT. Phase-based video motion processing. *ACM Trans Graphics*. 2013;32(4):1–9. https://doi.org/10.1145/2461912.2461966
29. Yang Y, Dorn C, Mancini T, et al. Reference-free detection of minute, non-visible, damage using full-field, high-resolution mode shapes output-only identified from digital videos of structures. *Struct Health Monit*. 2017;17(3):514-531. https://doi.org/10.1177/1475921717704385
30. Baqersad J, Poozesh P, Niezrecki C, Avitabile P. Photogrammetry and optical methods in structural dynamics—a review. *Mech Syst Signal Process*. 2017;86:17-34. https://doi.org/10.1016/j.ymssp.2016.02.011
31. Ha NS, Vang HM, Goo NS. Modal analysis using digital image correlation technique: An application to artificial wing mimicking beetle's hind wing. *Exp Mech*. 2015;55(5):989-998. https://doi.org/10.1007/s11340-015-9987-2
32. Molina-Viedma ÁJ, López-Alba E, Felipe-Sesé L, Díaz FA. Full-field modal analysis during base motion excitation using high-speed 3D digital image correlation. *Measure Sci Technol*. 2017;28(10):105402–1-105402–10. https://doi.org/10.1088/1361-6501/aa7d87
33. Huňady R, Hagara M. A new procedure of modal parameter estimation for high- speed digital image correlation. *Mech Syst Signal Process*. 2017;93:66-79. https://doi.org/10.1016/j.ymssp.2017.02.010
34. Warren C, Niezrecki C, Avitabile P. Optical non-contacting vibration measurement of rotating turbine blades II. *Struct Dyn Renew Energy, Conf Proce Soc Exp Mech*. 2011;1(Dic):39-44. https://doi.org/10.1007/978-1-4419-9716-6
35. Reu PL, Rohe DP, Jacobs LD. Comparison of DIC and LDV for practical vibration and modal measurements. *Mech Syst Signal Process*. 2017;86:2-16. https://doi.org/10.1016/j.ymssp.2016.02.006
36. Ehrhardt DA, Allen MS, Yang S, Beberniss TJ. Full-field linear and nonlinear measurements using continuous-scan laser Doppler vibrometry and high speed three-dimensional digital image correlation. *Mech Syst Signal Process*. 2017;86:82-97. https://doi.org/10.1016/j.ymssp.2015.12.003
37. Zanarini A. Competing optical instruments for the estimation of full field FRFs. *Measurement*. 2019;140:100-119. https://doi.org/10.1016/j.measurement.2018.12.017
38. Huňady R, Pavelka P, Lengvarský P. Vibration and modal analysis of a rotating disc using high-speed 3D digital image correlation. *Mech Syst Signal Process*. 2019;121:201-214. https://doi.org/10.1016/j.ymssp.2018.11.024
39. Rizo-Patron S, Sirohi J. Operational modal analysis of a helicopter rotor blade using digital image correlation. *Exp Mech*. 2017;57(3):367-375. https://doi.org/10.1007/s11340-016-0230-6
40. Molina-Viedma AJ, Felipe-Sesé L, López-Alba E, Díaz F. High frequency mode shapes characterisation using digital image correlation and phase-based motion magnification. *Mech Syst Signal Process*. 2018;102:245-261. https://doi.org/10.1016/j.ymssp.2017.09.019
41. Molina-Viedma AJ, Felipe-Sesé L, López-Alba E, Díaz FA. 3D mode shapes characterisation using phase-based motion magnification in large structures using stereoscopic DIC. *Mech Syst Signal Process*. 2018;108:140-155. https://doi.org/10.1016/j.ymssp.2018.02.006
42. Chang YH, Wang W, Chang JY, Mottershead JE. Compressed sensing for OMA using full-field vibration images. *Mech Syst Signal Process*. 2019;129:394-406. https://doi.org/10.1016/j.ymssp.2019.04.031
43. Molina-Viedma ÁJ, Felipe-Sesé L, López-Alba E, Díaz FA. Comparative of conventional and alternative digital image correlation techniques for 3D modal characterisation. *Measurement*. 2020;151:107010–1-107010–8. https://doi.org/10.1016/j.measurement.2019.107101
44. Felipe-Sesé L, Díaz FA. Damage methodology approach on a composite panel based on a combination of fringe projection and 2D digital image correlation. *Mech Syst Signal Process*. 2018;101:467-479. https://doi.org/10.1016/j.ymssp.2017.09.002
45. Mendrok K, Uhl T. The application of modal filters for damage detection. *Smart Struct Syst*. 2010;6(2):115-133.

46. Mendrok K, Kurowski P. Operational modal filter and its applications. *Arch Appl Mech*. 2013;83(4):509-519. https://doi.org/10.1007/s00419-012-0700-y
47. Mendrok K, Wójcicki J, Uhl T. An application of operational deflection shapes and spatial filtration for damage detection. *Smart Struct Syst*. 2015;16(6):1049-1068. https://doi.org/10.12989/sss.2015.16.6.1049
48. Deraemaeker A, Preumont A. Vibration based damage detection using large array sensors and spatial filters. *Mech Syst Signal Process*. 2006;20(7):1615-1630. https://doi.org/10.1016/j.ymssp.2005.02.010
49. Meirovithc L, Baruh H. The implementation of modal filters for control of structures. *J Guid Control Dynam*. 1985;8(6):707-716. https://doi.org/10.2514/3.20045
50. Zhang Q, Allemang RJ, Brown DL. Modal Filter: Concept and Applications. *Proceedings of the 8th International Modal Analysis Conference (IMAC)*, Orlando (USA) 1990.
51. Schreier H, Orteu JJ, Sutton MA. *Image Correlation for Shape, Motion and Deformation Measurements*. Springer US: Boston, MA; 2009.
52. Pan B. Digital image correlation for surface deformation measurement: historical developments, recent advances and future goals. *Measure Sci Technol*. 2018;29(8):082001–1-082001–32. https://doi.org/10.1088/1361-6501/aac55b

How to cite this article: Molina-Viedma Ángel Jesús, Pieczonka L, Mendrok K, López-Alba E, Díaz FA. Damage identification in frame structures using high-speed digital image correlation and local modal filtration. *Struct Control Health Monit*. 2020;e2586. https://doi.org/10.1002/stc.2586